Restoring Shoulder Abduction in Individuals with Tetraplegia using an Intracortical Brain-Computer Interface and a Soft Wearable Robot

Kushaal Rao[1], Henry Jenkins[2], Jacob Gusman[2,3], Maarten C. Ottenhoff[2,3], Ruixiang Li[2], Alexander Acosta[4], Lucille Panagos[4], Andrew Dempsey[4], Shane Allcroft[2,5], Emilia K. Mann[6], James Arnold[6], David Pont-Esteban[6], Harrison Young[6], Umut Civici[6], Connor McCann[6], Conor Walsh[6], Daniel B. Rubin[4,7], John D. Simeral[5,2,3], Carlos E. Vargas-Irwin[1,3,5], and Leigh R. Hochberg[5,2,4,7,3]

2025 12th International IEEE/EMBS Conference on Neural Engineering (NER) | 979-8-3315-9626-2/25/$31.00 ©2025 IEEE | DOI: 10.1109/NER61569.2025.11588968

Abstract— **For individuals who have lost the use of the upper limb, brain-computer interfaces (BCIs) offer a means of restoring function by translating neural activity into control signals for assistive technologies. Soft wearable robots present a promising path to reanimating a user's own limb through a comfortable, clothing-like interface and offer unique advantages, including broad clinical applicability. Combining BCIs with soft wearable robots may enable the restoration of natural, intuitive upper limb movement in individuals with tetraplegia. Here, we demonstrate BCI-driven restoration of shoulder abduction and adduction in two individuals with cervical spinal cord injury using a textile-based soft wearable robot.**

Clinical relevance— **Intuitively controlled, soft wearable robots hold promise for reanimating the arm and hand for people with spinal cord injury, stroke, or ALS.**

*This work was supported by the Office of Research and Development, Rehabilitation RD Service, Department of Veterans Affairs (A4820R, A2295R, A3803R, N2864C), NIH NIDCD (U01DC017844, K23DCO21297), NIH NINDS (U01NS123101), AHA (19CSLOI34780000), the Cullen Education and Research Fund (CERF) Medical Engineering Prize for ALS, National Science Foundation (2345107), and the National Science Foundation Graduate Research Fellowship Program (J.A.)

[1]K. Rao and C. E. Vargas-Irwin are with Department of Neuroscience, Brown University, Providence, Rhode Island. kushaal_rao@brown.edu

[2]H. Jenkins, J. Gusman, M. C. Ottenhoff, R. Li, S. Allcroft, and L. R. Hochberg are with School of Engineering, Brown University, Providence, Rhode Island.

[3]J. Gusman, M. C. Ottenhoff, C. E. Vargas-Irwin, and L.R. Hochberg are with Robert J. and Nancy D. Carney Institute for Brain Science, Brown University, Providence, Rhode Island

[4]A. Acosta, L. Panagos, A. Dempsey, D. B. Rubin, L. R. Hochberg are with Center for Neurotechnology and Neurorecovery, Dept of Neurology, Massachusetts General Hospital, Boston, Massachusetts

[5]S. Allcroft, C. E. Vargas-Irwin, and L. R. Hochberg are with Center for Neurorestoration and Neurotechnology, VA Providence Healthcare, Providence, Rhode Island

[6]E. K. Mann, J. Arnold, D. Pont-Esteban, H. Young, U. Civici, C. McCann, C. Walsh are with John A. Paulson School of Engineering and Applied Sciences, Harvard University, Cambridge, Massachusetts

[7]D. B. Rubin and L. R. Hochberg are with Department of Neurology, Harvard Medical School, Boston, Massachusetts

The study is performed under an Investigational Device Exemption from the U.S. Food and Drug Administration, is coordinated by the Center for Neurotechnology and Neurorecovery at Massachusetts General Hospital and is approved by the Mass General Brigham IRB (protocol : 2009P000505; CAUTION: Investigational Device. Limited by Federal Law to Investigational Use. The contents do not represent the views of the National Institutes of Health or the Department of Veterans Affairs or the United States Government).

I. INTRODUCTION

Paralysis caused by stroke, spinal cord injury, or neurodegenerative diseases such as amyotrophic lateral sclerosis (ALS) can severely impair independence and quality of life [1]. Among individuals living with tetraplegia, the restoration of arm and hand function is the most frequently expressed goal [2].

Intracortical brain-computer interfaces (iBCIs) can restore upper limb movement by translating neural activity into control signals for assistive devices. Prior studies have shown that individuals with tetraplegia can use iBCIs to perform reach and grasp tasks using technologies such as external anthropomorphic robotic limbs [3], [4], [5] or functional electrical stimulation (FES) [6], [7]. Although external robotic limbs have been widely studied for BCI control, their use remains limited due to unintuitive control schemes and a lack of native sensory feedback, which can reduce embodiment [8], [9], [10]. FES directly addresses these challenges by reanimating the user's own limb through electrical stimulation of muscles, allowing for intuitive, body-referenced control. However unlike robotic limbs that are externally actuated, the effectiveness of FES is constrained by rapid muscle fatigue and limited force production to overcome gravity, and it is not viable for individuals with motor neuron degeneration or muscle denervation, as occurs in ALS.

Soft wearable robots combine the external actuation benefits of robotic limbs with the intuitive, body-based control scheme and sensory feedback supported by FES. Constructed from compliant, flexible materials, these systems conform to the body and enable more natural, egocentric movement compared to rigid, externally positioned robotic arms. By mechanically actuating the user's limb, soft wearable robots can leverage intact sensory pathways to provide proprioceptive and other natural, somatosensory feedback and promote a more embodied user experience.

As an initial step, in this study, we demonstrate neural control of a textile-based, pneumatically actuated soft wearable robot (SWR) to restore shoulder abduction and adduction in individuals with tetraplegia. The SWR was initially designed to support shoulder abduction and adduction in individuals with stroke or ALS who retained some voluntary shoulder movement, relying on onboard sensors to detect residual motion for control [11]. To extend its use to individuals with complete paralysis of the arm, we adapted the system for direct control via an iBCI, eliminating the need for any overt movements. By decoding intended movements solely from neural activity, participants achieved real-time continuous control of their own shoulder motion through the SWR.

II. Methods

A. Participants

Two participants enrolled in the BrainGate2 pilot clinical trial (NCT00912041) participated in this research. Participant T18 is a 48 year-old right-handed man with tetraplegia resulting from a cervical spinal cord injury (C4 AIS-A) that occurred approximately 18 months prior to trial enrollment. He has four 64-electrode microelectrode arrays (Blackrock Microsystems; 1.5 mm electrode length) placed in the dorsal precentral gyrus (area 6d) of the left (motor dominant) hemisphere and two 64-electrode microelectrode arrays placed in the dorsal precentral gyrus (area 6d) of the right hemisphere. T18 has no residual movements below his site of injury but has limited sensation in his shoulders. Participant T11 is a 40 year-old right-handed man with tetraplegia resulting from a cervical spinal cord injury (C4 AIS-B) that occured approximately 11 years prior to trial enrollment. He has two 96-electrode microelectrode arrays placed in the dorsal precentral gyrus (area 6d) of the left hemisphere. T11 has some residual capacity to abduct his shoulder and flex his elbow but cannot reliably elicit any hand movements.

B. Soft Wearable Robot

The SWR is a fully portable, lightweight, textile-based, pneumatically actuated assistive device that enables shoulder abduction and adduction [12]. The actuator is anchored to the shirt and positioned along the lateral torso, extending from the ribcage up to the underside of the upper arm near the brachialis. It lies flush against the body to support shoulder abduction by generating an upward force when pressurized. Shoulder adduction occurs through passive deflation of the actuator and the assistance of gravity. The pneumatic supply, power, and electronics to control the system are embedded in a portable control box that can potentially be attached to a wheelchair. Four IMU sensors were placed on the user's torso, upper arm, forearm, and contralateral arm to measure the joint angles of the upper limb. They were daisy chained and streamed in real-time through a controller area network interface on the microcomputer in the SWR's control box.

C. Task Paradigm

Participants engaged in a custom Unity-based task ("PostureTrack") in which they controlled the shoulder of a virtual anthropomorphic avatar to track a continuously moving target. The avatar's movement reflected the single degree of freedom (DOF) enabled by the SWR: shoulder abduction and adduction. Target angles spanned five discrete positions, selected by a clinician based on each participant's available range of motion—60° to 85° for T11 and 52° to 73° for T18. Targets were presented in a randomized sequence, with each unique transition between angle pairs occurring exactly once, yielding 21 distinct paths (trials) per block. Each target position was held for four seconds before progressing, resulting in blocks lasting approximately two minutes. The avatar was displayed in beige by default and changed to green when the shoulder angle was within $\pm$ 2.5 degrees of the target, providing visual confirmation of accurate alignment (Fig. 2A). The PostureTrack task was displayed on a 32" monitor positioned approximately five feet in front of the participant. The perspective was set to a third-person, non-mirrored view from behind the avatar to facilitate imitation of movements. This allowed the participant to see the avatar's right side correspond to their own right side, and it also provided a clear view of the avatar's full range of arm motion.

Each research session began with participants completing two blocks of the PostureTrack task in a virtual condition to evaluate decoder performance in the absence of physical system dynamics. Following the two virtual blocks, participants donned the SWR and completed several blocks of the PostureTrack task for the SWR condition. The SWR was controlled using an iBCI that decoded intended movement from neural activity during attempted shoulder motions. IMU sensors mounted on the participant's body provided real-time estimates of shoulder abduction angle. In this condition, the avatar's shoulder position was updated based on IMU data, enabling real-time mapping of the participant's physical shoulder movements onto the virtual avatar. Data used for this analysis include two virtual and seven SWR blocks completed by T11 and two virtual and six SWR blocks completed by T18.

D. Neural Signal Processing and Decoding

We implemented a 1D rapidly-calibrating Kalman filter to achieve closed-loop control of shoulder abduction using the SWR.

1) Feature Extraction and Preprocessing: Neural voltage time series signals were recorded from each electrode with a sampling rate of 30 kHz, acquired using a Blackrock Neurotech NeuroPort system. Raw neural signals were filtered between 250-5000 Hz using a non-causal fourth order Butterworth filter. Linear regression referencing [13] filter coefficients and subsequent electrode-specific thresholds were determined using the filtered, digitized data recorded in an initial reference block at the beginning of the research session. Neural features used for closed-loop control included threshold crossings (putative action potentials) and spike-band power from every 1 ms window of filtered and denoised neural signals. Threshold crossings were identified for each electrode if the voltage of the signal in this 1 ms window crossed the threshold of -3.5 times the root mean squared value of the neural signal for that electrode. Spike-band power was obtained by squaring the voltage and averaging them over a 1 ms window for each electrode. These neural features were then binned into 20 ms non-overlapping bins. Binned threshold crossing counts were obtained by summing threshold crossings in 20 consecutive

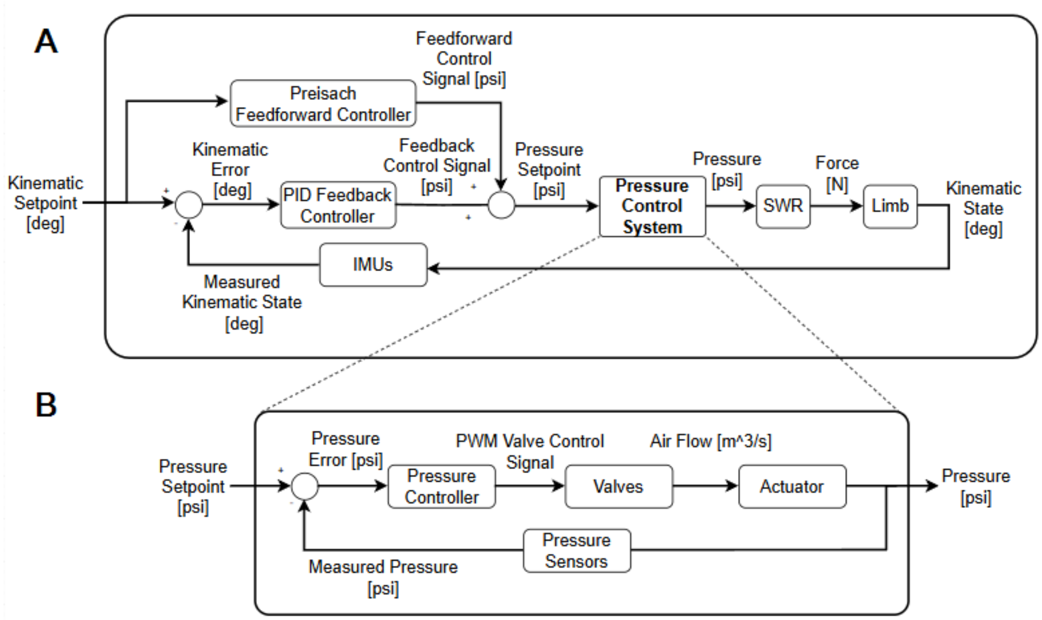

Fig. 1. (**A**) High-level kinematic control system consisting of a feedforward Preisach hysteresis model and a PID feedback controller. (**B**) Low-level pressure control system to modulate airflow to the SWR.

1 ms windows. Binned spike-band power was computed by averaging spike-band power in 20 consecutive neural feature windows. Finally, each feature was normalized using the z-score (mean subtracted and divided by standard deviation per feature) over a rolling 1 minute window to account for neural nonstationarities.

2) Rapidly Calibrating Kalman Decoder: Our lab has previously developed a rapidly calibrating Kalman filter that enables closed-loop control within seconds of decoder initialization [14]. In short, the rapid calibration framework runs a decoder and an updater in parallel. After calibration has been initialized at the beginning of a block, the updater trains a new decoder every 3 seconds on all available neural data, up to the most recent 3 minutes. The decoder's parameters are then updated by the updater and used to decode velocities. This approach eliminates the need for a dedicated open-loop block, often lasting several minutes, and allows for a rapid, seamless transition to closed-loop control. We adapted this framework to develop a 1D Kalman filter for shoulder abduction and adduction. Neural data was first collected during a 20-second open-loop calibration period, during which participants were shown two angular targets positioned in opposing directions relative to the starting position, each presented for 10 seconds. Participants were instructed to attempt shoulder abduction or adduction toward the displayed target during this period. Following this brief open-loop phase, the system transitioned seamlessly to closed-loop control, with participants controlling the SWR through their decoded neural activity for the remainder of the block. A new rapidly calibrating 1D Kalman filter was re-initialized at the beginning of each block, in both the virtual and SWR conditions.

E. Controller Design for the Soft Wearable Robot

We implemented a cascade control architecture consisting of a high-level kinematic controller and a low-level pressure controller (Fig. 1).

1) Kinematic Controller: Neural signals are decoded into angular velocity commands and then scaled to calculate changes in intended angular position, which serve as the reference signal for the kinematic controller. A feedforward Preisach hysteresis model [15] predicts the pressure needed to achieve the kinematic setpoint. In parallel, gain-scheduled proportional-integral-derivative (PID) feedback controller corrects for model inaccuracies and disturbances, using IMU readouts from the SWR to adjust the pressure command to the low-level pressure controller.

2) Pressure Controller: The low-level pressure controller uses proportional-derivative (PD) feedback control to command the valve states inside the control box, thereby modulating airflow to adjust actuator pressure. Pressure sensors are embedded in the control box in the compartment associated with each actuator to enable closed-loop feedback control. Pressure is also controlled in the upstream accumulator compartment to ensure adequate resources for control efforts with the SWR.

III. Results

In both the virtual and SWR experimental conditions, both participants demonstrated accurate neural control of shoulder abduction within seconds following the initial 20 s calibration period of each block. Participants T18 and T11 consistently reached and held the target posture within a ± 2.5 degree tolerance during the 4-second dwell period (Fig. 2C). For T18, trial success rates were 90.48% in the virtual condition (2 blocks) and 86.43% with the SWR (6

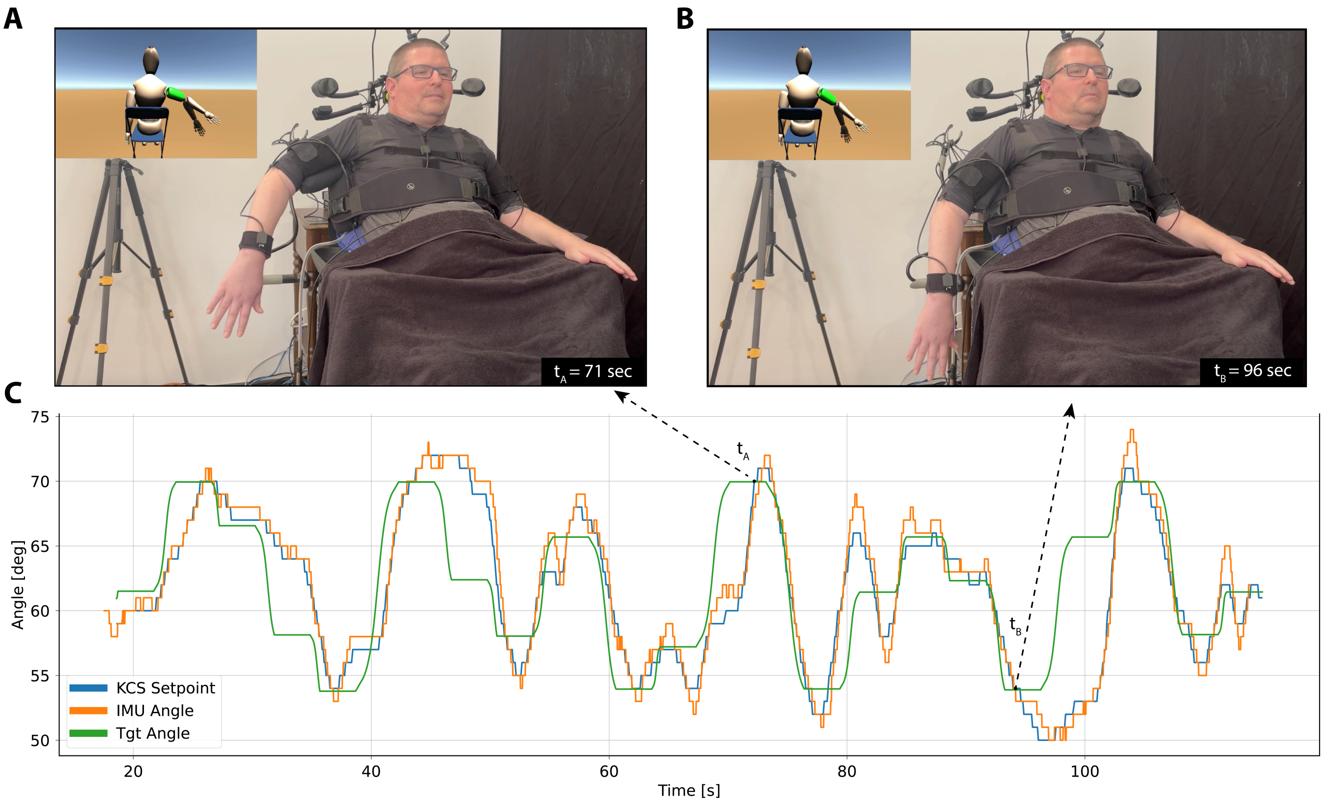

Fig. 2. SWR condition of the PostureTrack task performed by T18 with the SWR donned on his right shoulder. **A**) Successful acquisition (inset, shoulder highlighted in green) of virtual target at 70 degrees of shoulder abduction via physical movement of SWR (t_A). (**B**) Successful acquisition (inset, shoulder highlighted in green) of virtual target at 53 degrees of shoulder abduction via physical movement of SWR t_B). (**C**) Time-series representation of a representative block of the PostureTrack task following the calibration period. Traces represent the decoded angle (blue), achieved angle (orange), and target angle (green). Annotations t_A and t_B correspond to panels A and B. Avatar shoulder and elbow angle are driven by IMU output; only shoulder angle is controlled by SWR, which is reflected in the exclusive coloring of the shoulder joint.

blocks). For T11, success rates were 85.71% in the virtual condition (2 blocks) and 56.03% in the physical condition (7 blocks).

As expected, tracking performance was higher in the virtual condition than in the SWR condition, likely due to the additional delay introduced by moving the physical arm with the pneumatically actuated device. For T18, the root mean squared error (RMSE) between the avatar's shoulder angle and the target trajectory was lower in the virtual condition (2.41 ± 0.10 degrees, mean ± std) compared to the SWR condition (5.46 ± 0.56 degrees), where the avatar reflected the participant's actual shoulder movement. A similar trend was observed for T11, with an RMSE of 5.94 ± 0.33 degrees in the virtual condition and 11.76 ± 2.68 degrees in the SWR condition.

To better understand potential sources of tracking error in the SWR condition, we also evaluated the performance of the SWR's high-level kinematic controller by comparing the controller's reference signal—the desired shoulder angle output from the neural decoder—to the measured shoulder angle recorded by the IMU sensors on the SWR. The RMSE between these signals was 1.56 ± 0.68 degrees for T18 and 5.82 ± 2.48 degrees for T11, suggesting that both physical system delays and additional control system error may have contributed to increased tracking error in the SWR condition of the PostureTrack task.

In addition to assessing continuous tracking error, we also examined posture stability during the dwell period of all successful trials. For T18, RMSE during the dwell period was 2.61 ± 0.27 degrees in the virtual condition and 5.87 ± 1.42 degrees in the SWR condition (Fig. 3B). For T11, RMSE was 6.92 ± 1.63 degrees in the virtual condition and 11.25 ± 2.68 degrees in the SWR condition (Fig. 3A). These values suggest that while participants were able to maintain a target posture within the ± 2.5 degree target zone in a majority of trials, remaining stationary in the SWR condition was considerably more challenging.

Finally, cross-correlation analysis between the target trajectory and the SWR's IMU angle revealed a negative lag, indicating that the SWR movements lagged behind the reference target. This delay is attributable to a combination of factors, including the SWR's system dynamics, communication latency between the BCI and the SWR, and the participant's reaction time. The analysis was a full cross-correlation, examining the full space of possible lags within each 2 minute block. For T18, the peak correlation was $r = 0.64 \pm 0.10$ (mean ± std) at a lag of -1.36 ± 0.29 seconds in the SWR condition and $r = 0.96 \pm 0.00$ at a lag

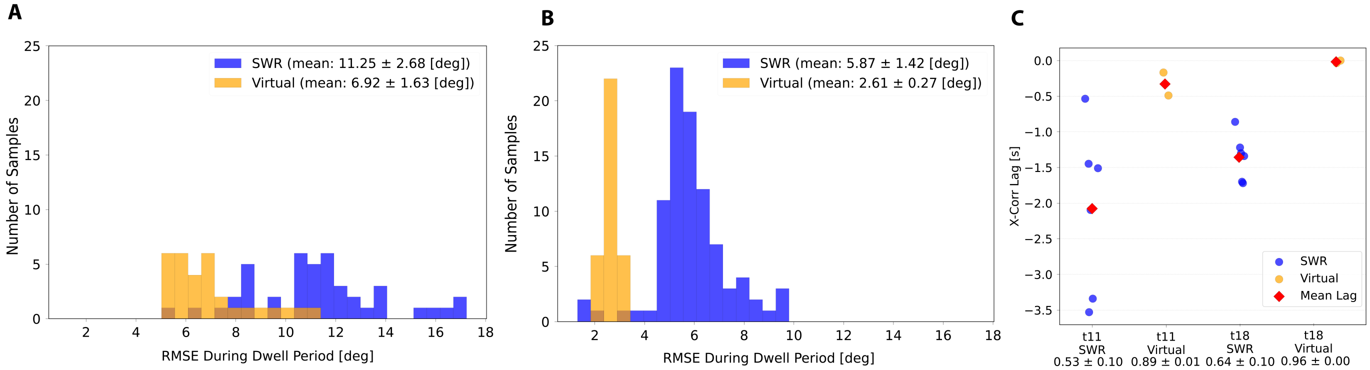

Fig. 3. Performance metrics during virtual and SWR conditions of the PostureTrack task. (**A**) T11 and (**B**) T18: RMSE distributions during the dwell period of successful trials in the SWR and virtual condition of the PostureTrack task. (**C**) Cross-correlation lag for each block of the PostureTrack task, shown separately for each participant and condition. The red diamond indicates the mean lag, and the mean correlation coefficient is labeled below each column.

of -0.02 ± 0.02 seconds in the virtual condition. For T11, the peak correlation was $r = 0.53\pm0.10$ at a lag of -2.08 ± 1.06 seconds in the SWR condition, and $r = 0.89 \pm 0.01$ at a lag of -0.33 ± 0.16 seconds in the virtual condition (Fig. 3C).

IV. Discussion

In this study, we present a novel approach for restoring voluntary movement to a paralyzed limb by integrating an iBCI with an SWR. Two participants enrolled in the BrainGate2 clinical trial achieved continuous control of shoulder abduction and adduction within 20 seconds of decoder initialization, enabled by a rapidly calibrating Kalman filter trained on neural activity recorded from the precentral gyrus. Decoded neural signals were passed into a high-level kinematic control system, comprising a feedforward Preisach hysteresis model and a PID feedback controller. These findings highlight the potential of iBCI-controlled soft wearable robotics to restore intuitive upper limb function in individuals with tetraplegia by overcoming key limitations of prior technologies: it is broadly applicable to a wider range of users than FES, and by leveraging preserved sensory feedback and egocentric control, it promotes greater embodiment and more naturalistic control than traditional robotic limbs.

However, restoring physical movement through soft robotics also presents unique challenges not encountered in virtual BCI applications such as speech decoding, cursor control, or text entry. These tasks occur in purely digital environments, where system responses are immediate and unconstrained by physical dynamics. In contrast, movement restoration involves controlling systems with complex physical behavior. The textile-based composition of soft wearable robots and its associated pneumatic actuation introduces additional control complexities, including nonlinearities, hysteresis, and variable compliance—factors largely absent in virtual domains and less pronounced in rigid robotic systems.

These physical characteristics create a dual-layered uncertainty for the user. In standard BCI systems, uncertainty primarily arises from the mapping between neural activity and decoder output. However, in the context of movement restoration, a second layer of uncertainty emerges in the translation of the decoder's output into changes in physical state. Here, the decoder serves not as the system's endpoint, but as a command input to a downstream control system. As a result, user feedback reflects both decoding uncertainty and variability in the robot's kinematic response, potentially complicating the development of stable and intuitive control strategies. This layered uncertainty likely contributes to the discrepancy in performance between the virtual and SWR conditions of the PostureTrack task. Consistent with this interpretation, both participants exhibited increased RMSE and a longer lag time to peak correlation in the SWR condition compared to the virtual condition. Including both conditions allowed us to isolate performance differences attributable to the SWR's inherent characteristics—such as its pneumatic actuator dynamics, communication latency, and compounded uncertainty in the feedback received by the participant.

A further challenge in wearable robotics lies in accommodating inter-individual variability in residual motor function. Participant T18 exhibited no volitional movement below the level of injury and only limited shoulder sensation, whereas T11 retained some ability to abduct the shoulder and flex the elbow. We hypothesize that differences in controller RMSE between participants—despite the use of an identical control architecture—reflect T11's residual voluntary efforts. These motor attempts may have introduced discrepancies between intended and actual motion, leading to deviations from the decoder's reference trajectory and therefore increased tracking error. Future control scheme implementations may explore personalized adaptation to the user's residual motor function.

In conclusion, we demonstrate that neural control of soft wearable robots can restore shoulder abduction and adduction in two people with cervical spinal cord injury. Future work will focus on expanding neural control from single to multi-joint SWRs for the upper limb to enable coordinated reach and grasp movements within a 3D workspace, and further testing with clinical trial participants with other causes of paralysis (e.g., brainstem stroke, ALS). As additional DOFs are introduced to the SWR, the effects of hysteresis, nonlinearities, and coupled dynamics may be further amplified, potentially compounding control challenges. Coupling multi-DOF soft robotic systems with robust neural decoding strategies will be critical for translating this technology into meaningful functional restoration for individuals with severe motor impairments.

ACKNOWLEDGMENT

We thank participants T18, T11, and their carepartners for their time, dedication, and contributions towards this research. We thank Maryam Masood, Dave Rosler, and Beth Travers for their regulatory and team management efforts supporting this work. We thank undergraduates Benjamin Schornstein for early iterations towards developing the custom Unity-based task and Richard Cheng for sensor characterization and integration.

REFERENCES

[1] M. Dijkers, "Quality of life after spinal cord injury: a meta analysis of the effects of disablement components," *Spinal Cord*, vol. 35, no. 12, pp. 829–840, Dec. 1997.

[2] K. D. Anderson, "Targeting recovery: Priorities of the spinal cord-injured population," *Journal of Neurotrauma*, vol. 21, no. 10, pp. 1371–1383, 2004. [Online]. Available: https://doi.org/10.1089/neu.2004.21.1371

[3] L. R. Hochberg, D. Bacher, B. Jarosiewicz, N. Y. Masse, J. D. Simeral, J. Vogel, S. Haddadin, J. Liu, S. S. Cash, P. van der Smagt, and J. P. Donoghue, "Reach and grasp by people with tetraplegia using a neurally controlled robotic arm," *Nature*, vol. 485, no. 7398, pp. 372–375, May 2012. [Online]. Available: https://www.ncbi.nlm.nih.gov/pmc/articles/PMC3640850/

[4] J. L. Collinger, B. Wodlinger, J. E. Downey, W. Wang, E. C. Tyler-Kabara, D. J. Weber, A. J. C. McMorland, M. Velliste, M. L. Boninger, and A. B. Schwartz, "High-performance neuroprosthetic control by an individual with tetraplegia," *Lancet (London, England)*, vol. 381, no. 9866, pp. 557–564, Feb. 2013.

[5] N. Natraj, S. Seko, R. Abiri, R. Miao, H. Yan, Y. Graham, A. Tu-Chan, E. F. Chang, and K. Ganguly, "Sampling representational plasticity of simple imagined movements across days enables long-term neuroprosthetic control," *Cell*, vol. 188, no. 5, pp. 1208–1225.e32, Mar. 2025.

[6] A. B. Ajiboye, F. R. Willett, D. R. Young, W. D. Memberg, B. A. Murphy, J. P. Miller, B. L. Walter, J. A. Sweet, H. A. Hoyen, M. W. Keith, P. H. Peckham, J. D. Simeral, J. P. Donoghue, L. R. Hochberg, and R. F. Kirsch, "Restoration of reaching and grasping movements through brain-controlled muscle stimulation in a person with tetraplegia: a proof-of-concept demonstration," *The Lancet*, vol. 389, no. 10081, pp. 1821–1830, May 2017, publisher: Elsevier. [Online]. Available: https://www.thelancet.com/journals/lancet/article/PIIS0140-6736(17)30601-3/abstract?elsca1=tlpr

[7] C. E. Bouton, A. Shaikhouni, N. V. Annetta, M. A. Bockbrader, D. A. Friedenberg, D. M. Nielson, G. Sharma, P. B. Sederberg, B. C. Glenn, W. J. Mysiw, A. G. Morgan, M. Deogaonkar, and A. R. Rezai, "Restoring cortical control of functional movement in a human with quadriplegia," *Nature*, vol. 533, no. 7602, pp. 247–250, May 2016, publisher: Nature Publishing Group. [Online]. Available: https://www.nature.com/articles/nature17435

[8] F. Cordella, A. L. Ciancio, R. Sacchetti, A. Davalli, A. G. Cutti, E. Guglielmelli, and L. Zollo, "Literature Review on Needs of Upper Limb Prosthesis Users," *Frontiers in Neuroscience*, vol. 10, p. 209, 2016.

[9] K. L. Collins, A. Guterstam, J. Cronin, J. D. Olson, H. H. Ehrsson, and J. G. Ojemann, "Ownership of an artificial limb induced by electrical brain stimulation," *Proceedings of the National Academy of Sciences of the United States of America*, vol. 114, no. 1, pp. 166–171, Jan. 2017.

[10] S. N. Flesher, J. E. Downey, J. M. Weiss, C. L. Hughes, A. J. Herrera, E. C. Tyler-Kabara, M. L. Boninger, J. L. Collinger, and R. A. Gaunt, "A brain-computer interface that evokes tactile sensations improves robotic arm control," *Science (New York, N.Y.)*, vol. 372, no. 6544, pp. 831–836, May 2021.

[11] T. Proietti, C. O'Neill, L. Gerez, T. Cole, S. Mendelowitz, K. Nuckols, C. Hohimer, D. Lin, S. Paganoni, and C. Walsh, "Restoring arm function with a soft robotic wearable for individuals with amyotrophic lateral sclerosis," *Science Translational Medicine*, vol. 15, no. 681, p. eadd1504, Feb. 2023, publisher: American Association for the Advancement of Science. [Online]. Available: https://www.science.org/doi/10.1126/scitranslmed.add1504

[12] T. Proietti, C. O'Neill, C. J. Hohimer, K. Nuckols, M. E. Clarke, Y. M. Zhou, D. J. Lin, and C. J. Walsh, "Sensing and Control of a Multi-Joint Soft Wearable Robot for Upper-Limb Assistance and Rehabilitation," *IEEE Robotics and Automation Letters*, vol. 6, no. 2, pp. 2381–2388, Apr. 2021. [Online]. Available: https://ieeexplore.ieee.org/document/9360430

[13] D. Young, F. Willett, W. D. Memberg, B. Murphy, B. Walter, J. Sweet, J. Miller, L. R. Hochberg, R. F. Kirsch, and A. B. Ajiboye, "Signal processing methods for reducing artifacts in microelectrode brain recordings caused by functional electrical stimulation," *Journal of Neural Engineering*, vol. 15, no. 2, p. 026014, Apr. 2018.

[14] D. M. Brandman, T. Hosman, J. Saab, M. C. Burkhart, B. E. Shanahan, J. G. Ciancibello, A. A. Sarma, D. J. Milstein, C. E. Vargas-Irwin, B. Franco, J. Kelemen, C. Blabe, B. A. Murphy, D. R. Young, F. R. Willett, C. Pandarinath, S. D. Stavisky, R. F. Kirsch, B. L. Walter, A. Bolu Ajiboye, S. S. Cash, E. N. Eskandar, J. P. Miller, J. A. Sweet, K. V. Shenoy, J. M. Henderson, B. Jarosiewicz, M. T. Harrison, J. D. Simeral, and L. R. Hochberg, "Rapid calibration of an intracortical brain-computer interface for people with tetraplegia," *Journal of Neural Engineering*, vol. 15, no. 2, p. 026007, Apr. 2018.

[15] C. M. McCann, J. Arnold, C. Lehmacher, K. Bertoldi, and C. J. Walsh, "On-body textile hysteresis estimation for personalized physical human-robot interaction," *The International Journal of Robotics Research*, p. 02783649251358840, Jul. 2025, publisher: SAGE Publications Ltd STM. [Online]. Available: https://doi.org/10.1177/02783649251358840